

Monotonic and cyclic components of radio pulsars spin-down

A. Biryukov^{1*}, G. Beskin^{2†}, S. Karpov²

¹*Sternberg Astronomical Institute of MSU, 13 Universitetsky pr., Moscow, 119992, Russia*

²*Special Astrophysical Observatory of RAS, Nizhnij Arkhyz, Karachaevo-Cherkesia, 369167, Russia*

Accepted . Received ; in original form

ABSTRACT

In this article we revise the problem of anomalous values of pulsars’ braking indices n_{obs} and frequency second derivatives $\ddot{\nu}$ arising in observations. The intrinsic evolutionary braking is buried deep under superimposed irregular processes, that prevent direct estimations of its parameters for the majority of pulsars. We re-analyze the distribution of “ordinary” radio pulsars on a $\ddot{\nu} - \dot{\nu}$, $\ddot{\nu} - \nu$, $\dot{\nu} - \nu$ and $n_{obs} - \tau_{ch}$ diagrams assuming their spin-down to be the superposition of a “true” monotonous term and a symmetric oscillatory term. We demonstrate that their effects may be clearly separated using simple *ad hoc* arguments. Using maximum likelihood estimator we derive the parameters of both components. We find characteristic timescales of such oscillations to be of the order of $10^3 - 10^4$ years, while its amplitudes are large enough to modulate the observed spin-down rate up to 0.5-5 times and completely dominate the second frequency derivatives. On the other hand, pulsars’ secular evolution is consistent with classical magnetodipolar model with braking index $n \approx 3$

So, observed pulsars’ characteristic ages (and similar estimators that depend on the observed $\dot{\nu}$) are also affected by long term cyclic process and differ up to 0.5-5 times from their monotonous values. This fact naturally resolves the discrepancy of characteristic and independently estimated physical ages of several objects, as well as explains very large, up to 10^8 years, characteristic ages of some pulsars.

We discuss the possible physical connection of long term oscillation with a complex neutron star rotation relative its magnetic axis due to influence of the near-field part of magnetodipolar torque.

Key words: stars: pulsars: general – methods: statistical
PACS 04.40.Dg – 95.75.Pq – 97.60.Gb – 98.62.Ve

1 INTRODUCTION

Radio pulsars are highly periodic variable astrophysical objects, powered by neutron stars’ rotation with periods evolving with time. Observational determination of their timing parameters – instantaneous period and its derivatives – is an extremely complex task (Edwards et al. 2006; Cordes & Shannon 2010), but after the correction of pulse times of arrivals (TOAs) for the effects of radio wave propagation in the interstellar medium, motion and position of the Earth, gravitational delays in Solar system potential etc., the resulting phase of the light curve may be well described

by an (infinite) Taylor series

$$\phi(t) = \phi_0 + \nu(t - t_0) + \frac{1}{2}\dot{\nu}(t - t_0)^2 + \frac{1}{6}\ddot{\nu}(t - t_0)^3 + \dots \quad (1)$$

dominated by the lower order terms. This may also be expressed in terms of observed rotational frequency as

$$\nu(t) = \nu_0 + \dot{\nu}(t - t_0) + \frac{1}{2}\ddot{\nu}(t - t_0)^2 + \frac{1}{6}\ddot{\nu}(t - t_0)^3 + \dots \quad (2)$$

where values of ν and its derivatives are attributed to the epoch t_0 .

At the same time, the majority of published theoretical models of pulsar braking predict the spin-down described by a differential equation of the form (Manchester & Taylor 1977; Beskin et al. 1993)

$$\dot{\nu} = -K\nu^n, \quad (3)$$

where n is a (constant) braking index and K depends on the

* E-mail: eman@sai.msu.ru

† E-mail: beskin@sao.ru

individual physical properties of the pulsar. For the vacuum magnetodipolar model the canonical value is $n = 3$, pulsar wind decreases it to $n = 1$ and multipole magnetic field increases it to $n \geq 5$ (Manchester & Taylor 1977).

For such a spin-down with *constant* K the braking index is equal to a simple combination of frequency and two its derivatives¹

$$n_{obs} = \frac{\nu\ddot{\nu}}{\dot{\nu}^2} = n \quad (4)$$

That is why the determination of spin frequency second derivative via pulsar timing is important for understanding the pulsar's spin-down.

Several decades of very detailed timing of hundreds of pulsars (D'Alessandro et al. 1993; Baykal et al. 1999; Chukwude 2003; Hobbs et al. 2004, 2010; Livingstone et al. 2005), including the best studied one – Crab pulsar (Scott et al. 2003) – demonstrated, however, that the measured rotational phase (1) evolution is not generally consistent with the one expected for a braking law (3) with physically reasonable parameters. Observed rotational phase ϕ (as well as ν , $\dot{\nu}$) includes components with a very complex, irregular behaviour. The first kind of such irregularities is “glitches” – sporadic fast changes of pulsars' periods and spin-down rate with up to few months relaxation timescale (e.g. Manchester & Taylor (1977)), while the other one – quasi-random phase variations with typically red Fourier spectrum and characteristic timescales of a few months to few years – “timing noise” (e.g. Cordes & Helfand (1980); Lyne (1999); Hobbs et al. (2010)).

Both of them affect the measurements of ν , $\dot{\nu}$ and $\ddot{\nu}$, and often make them dependent on the duration and epoch t_0 of the observations' time span, when it is shorter or comparable to timescales of these processes. But, if observations are performed over sufficiently long intervals of about a decade or longer, the observed coefficients of series (1) become more stable – the influence of these irregularities is mostly suppressed (see Sec. 2.1 for additional discussion). To date, there are more than 200 pulsars observed for longer than 15 years (Baykal et al. 1999; Chukwude 2003; Hobbs et al. 2004, 2010), and still the majority of $\ddot{\nu}$ values, measured over such long intervals, lead to extremely high, up to 10^6 (and even more), braking indices. Moreover, their values are negative for nearly a half of all objects. In general, measured braking indices drastically differ from physically reasonable values, and this raises serious problem on the pulsars' long term spin evolution.

While glitches are widely believed to be caused by a rapid transfer of momentum from the neutron stars interior (e.g. Espinoza et al. (2011) and references therein), the nature of the timing noise is still unclear and no self-consistent and widely accepted model of pulsars' phase residuals irregularities is constructed. There have been numerous attempts to attribute it to various stochastic phenomena in the neutron star magnetosphere (Cheng et al. 1987; Contopoulos 2007; Lyne et al. 2010), in the interior (Cordes & Downs

1985), to spin-down torque variations (Urama et al. 2006), and to the existence of a number of different spin-down regimes for a single pulsar (Lyne et al. 2010). Purely phenomenological attempts to describe observed noise as random walks of different orders (in phase, frequency or its derivative) (Cordes & Greenstein 1981) have also not succeeded as with the increase of observations time spans the noise appeared to be more complex than these simple models predict. Some characteristics of this essentially irregular process, however, have been parametrized through several noise strength parameters and their correlations. So, Arzoumanian et al. (1994) parametrized pulsars' timing noise through $\Delta_s \propto \log(|\ddot{\nu}|/\nu)$ quantity and found a good $\Delta_s - \dot{P}$ correlation, where P is a pulsar period.

In turn, Cordes & Helfand (1980), Cordes & Downs (1985) and then Chukwude (2003) have investigated activity parameter A , which is a direct measure of timing residuals variance. A good correlations of A versus $\dot{\nu}$ and $\ddot{\nu}$ was also found.

However, the quantities used in these papers to parametrize timing noise were in fact just the measures of observed frequency second derivative. Even the activity parameter A was calculated using timing residuals after subtraction of a second order polynomial in series (1). Therefore, the correlations obtained simply reflect the quite strong $\ddot{\nu} - \dot{\nu}$ dependence.

At the same time, only a few long-term mechanisms have been offered to explain observed anomalous braking indices. Demiański & Proszynski (1979) studied the variations of pulsar timing parameters due to existence of possible massive partner – most of radio pulsars are, however, believed to be isolated objects. Alpar & Baykal (2006) investigated the impact of unresolved or missed glitches on the observed timing parameters, but it is very difficult to explain some extremely high braking indices $|n| > 10^2 - 10^3$ by such mechanism. Gullahorn & Rankin (1977) considered variations of pulsar braking torque with timescales of $10^2 - 10^4$ years, probably due to interaction of the pulsar with interstellar medium in its vicinity. The idea of spin-down torque variations itself is quite promising and reasonable, but the nature of variations on such timescale was not pointed out in their note and remained unclear.

In turn, in Beskin et al. (2006) and Biryukov et al. (2007) we considered the existence of a long-term cyclic variational process affecting pulsars' spin-down on a timescale of thousands of years. One may call such a process a third type of timing irregularities. Later, Barsukov & Tsygan (2010) suggested that the physical nature of such a process may be related to the “anomalous” magnetodipolar braking torque, which may produce a forced precession of pulsar's rotational axis around its magnetic moment with the period of $10^3 - 10^4$ years, and demonstrated the possibility of significant variations of observed rotational parameters on such timescale. Even earlier, Melatos (2000) also investigated the triaxial neutron star rotation taking into account this torque and demonstrated that the rotation of such star may be very complex and even induce variations of magnetic inclination angle, which will also affect the neutron star spin-down.

As a further development of this concept of a long-term variational process, in the current work we analyse the ensemble of 297 pulsars with published data on second frequency derivatives and demonstrate that these values may

¹ Note that the *observed* ones, estimated by fitting the TOAs with a model of (1) broken down to the third order term, are always biased even if the spin-down is exactly according to equation (3) due to influence of non-zero higher-order terms. For actual pulsars, however, this bias is negligible and will be ignored below.

be used to estimate the parameters of both secular (evolutionary, monotonous) and additional, cyclic, components of a pulsar spin-down under simple and reasonable assumptions. We formulate such a two-component model of pulsar braking and derive its parameters using a maximum likelihood estimator. The results are quite reasonable, as the parameters of monotonous component are in a good agreement with a standard magnetodipolar spin-down model.

The article is organized as follows. In Section 2 we justify that measured $\ddot{\nu}$ values can indeed be used to analyse pulsars' spin-down. In Section 3, statistical analysis of a 297 objects is performed, phenomenology of a two-component pulsars' spin-down is presented and parameters of its irregular term are roughly estimated using model-independent arguments. In Section 4 this two-component model is used for the determination of the secular spin-down parameters also. In Section 5 we discuss the results and its astrophysical implications. The conclusions are given in Section 6.

2 PULSARS' $\ddot{\nu}$ MEASUREMENTS

2.1 What $\ddot{\nu}$'s can tell us on the pulsars' physics?

Anomalous values of $\ddot{\nu}$ (and braking indices) for most of ordinary pulsars raise at least two principal questions, critical for any serious analysis of these quantities. Namely:

- Are values measured over long timespans (decades) really related to pulsars' or interstellar medium² physics or they are just artifacts of somewhat incorrect observations and/or data reduction?

and

- If they are not artifacts, then is the anomaly induced by the same phenomena responsible for the short time scale (months) quasi-periodic timing irregularities with red-like spectra, observed in timing residuals?

The answer to the first question above is clear. Pulsar timing is a complex, but well-defined and thoroughly described procedure, and the sources of observational uncertainties arising in it are well known and are taken into account during the reduction, as well as various effects that affect the timing systematically – e.g. motion of the Earth, relativistic effects, etc (see, for example, Edwards et al. (2006)). There is no reason to believe the significant cubic trends, clearly seen in phase solutions for hundreds of pulsars (Hobbs et al. 2004), are artifacts.

There is also a method for indirect measurements of a pulsar' second derivative by comparing $\dot{\nu}$ values acquired over sufficiently distant, separated by 6–20 years, time spans (Johnston & Galloway 1999). Results of such estimation are anomalous too, and are generally consistent with directly measured values.

Obviously, all accurately measured $\ddot{\nu}$ values, even being anomalous, are physically meaningful – they are indeed due

to peculiarities of pulsars' spin down, while their anomalousness is just an indication of insufficiency of our models of pulsars' braking.

On the other hand, the answer to the second question is not so obvious, as stochastic timing irregularities, seen in a large fraction of pulsars, still are not well understood and are complex phenomena.

Phenomenologically, timing residuals' irregularities and unexpected anomalous parameters of timing solution have to be separated in the analysis. Indeed, the former ones are seen directly within observational datasets and their stochastic nature is clear while the origin of the latter ones can only be speculated about. Below we argue in favour of indeed different origins of these phenomena.

The phase residuals after all appropriate corrections and quadratic trend subtraction (i.e. after extraction of ν and $\dot{\nu}$ only) form a very plural zoo over the pulsar population. There are at least several different classes of typical pulsars' timing series (see Figure 3 in Hobbs et al. (2010)) – the ones with dominant influence of a cubic term (e.g. PSRs B0959-54, B0943+10, B1657-13 etc.), the ones with more complex but generally smooth behaviour (PSRs B1620-26, B1706-16, B1727-47 etc.), and the ones that are purely white noise supposedly due to measurement errors. The latter class typically contains pulsars with inaccurate or unmeasured second frequency derivatives, and will not be analysed here. The second one is often used to depict the timing deviations from an expected spin-down law as a process with red noise-like spectrum; there are, however, some evidences that this behaviour in fact is a combination of a cubic order term and a quasi-periodic component (Hobbs et al. 2010). Moreover, young pulsars (e.g. Crab, B1509-58, B2011+38) show strong short-term quasi-periodic timing noise, along with cubic trends corresponding to a spin-down with physically meaningful braking indices ~ 3 (Lyne et al. 1993; Scott et al. 2003; Livingstone et al. 2005; Hobbs et al. 2010).

Also, the behaviour of $\ddot{\nu}$'s with the increase of observational span is not consistent with their origin due to stochastic or short timescale noise processes. For example, for PSR B1706-16, variations of $\ddot{\nu}$ with an amplitude of 10^{-24} s^{-3} have been detected on a timescale of several years (see Figure 7 in Hobbs et al. (2004)) – its values, however, are always around the one revealed by the fit over the entire 25 year time span ($\ddot{\nu} = 3.8 \times 10^{-25} \text{ s}^{-3}$), which still leads to a braking index $\approx 2.7 \times 10^3$.

All this strongly suggest that timing noise is a process distinct from the one producing large (and anomalous) cubic trends in (1); this noise acts mostly as a randomizing factor decreasing the accuracy of $\ddot{\nu}$ measurements, but not defining their properties in general.

As a result, we believe the second derivative values to be very promising tool for studying long timescale features of pulsars' spin-down. Although the $\ddot{\nu}$ values of individual pulsars bring little information on the spin-down of neutron stars, the properties of its distribution over an *ensemble* of all pulsars seems to be appropriate for spin-down study under a simple and reasonable assumptions on the properties of process producing these anomalous cubic trends.

² The effects of propagation of pulsar radiation through its “near” and “far” medium can introduce an additional delays to the times of pulses arrivals and therefore affect the timing solution (Cordes & Lazio 2002; Cordes & Shannon 2010).

2.2 The subset

The set of pulsars under investigation is similar to the one used in our previous works (Beskin et al. 2006; Biryukov et al. 2007). From the 393 objects of the ATNF³ catalogue (Manchester et al. 2005) with known $\ddot{\nu}$ we have compiled a list of “ordinary” radio pulsars that

- have $P > 20$ ms and $|\dot{P}| > 10^{-17}$ s/s (i.e. had not been recycled);
- have relative accuracy of second derivative measurements better than 75%;
- are not components of binary systems and not in a list of known anomalous x-ray pulsars.

19 supplementary pulsars from other sources (D’Alessandro et al. 1993; Chukwude 2003) have been added. The final set consists of 297 objects including 247 from (Hobbs et al. 2004). 18 of them are associated with young supernova remnants⁴

3 STATISTICAL ANALYSIS OF PULSARS’ TIMING PARAMETERS

3.1 $\nu - \dot{\nu} - \ddot{\nu}$ dependency. Cyclic evolution of pulsars’ spin-down?

Our work is based on the study of relations between quantities derived from pulsars’ timing: spin frequency, its two derivatives $\dot{\nu}$ and $\ddot{\nu}$, observed braking index $n_{obs} = \ddot{\nu}\nu/\dot{\nu}^2$ and characteristic age $\tau_{ch} = -\nu/2\dot{\nu}$.

As we previously demonstrated in (Biryukov et al. 2007), the logarithms of $|\ddot{\nu}|$ show significant correlation with the ones of $-\dot{\nu}$ for both positive (172 pulsars, correlation coefficient $r \approx 0.9$) and negative (125 pulsars, $r \approx 0.82$) branches of the $\ddot{\nu} - \dot{\nu}$ diagram (Figure 1).

The apparent separation of branches on the $\ddot{\nu} - \dot{\nu}$ diagram is primarily due to the logarithmic scale of the plot, and actually objects continuously cover the full range of $\ddot{\nu}$ values, excluding only the gap on small ones due to limited accuracy of measurements (which is not better than 10^{-29} s⁻³).

Young pulsars confidently associated with supernova remnants are systematically shifted to the left on the diagram (open symbols in Figure 1) and are absent on the right. Hence, pulsars seem to evolve towards lower values of $|\dot{\nu}|$. Moreover, if τ_{ch} is an appropriate pulsar age estimator, then $|\dot{\nu}|$ is the same too, as they are highly correlated ($r = 0.99$ in logarithmic scale, see Fig. 5)

On the $\ddot{\nu} - \nu$ diagram, shown in Figure 3, pulsars’ behaviour is similar: they are born with higher values of ν and, since $\dot{\nu} < 0$, evolve toward lower values. The direction of the evolution is the same for positive and negative branches of $\ddot{\nu} - \nu$. So all older pulsars have systematically lower values of $|\ddot{\nu}|$ which is consistent with evolutionary interpretation of $\ddot{\nu} - \dot{\nu}$ diagram.

So, we conclude that each pulsar during its evolution moves along the branches of the $\ddot{\nu} - \dot{\nu}$ and $\ddot{\nu} - \nu$ diagrams

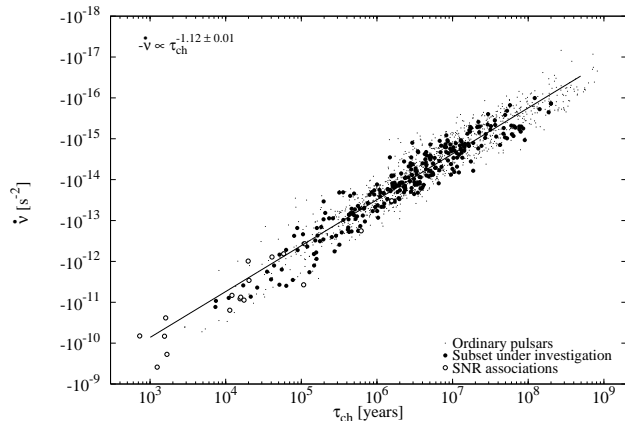


Figure 5. The correlation between $\dot{\nu}$ and characteristic age $\tau_{ch} = -\nu/2\dot{\nu}$ for 297 pulsars with measured $\ddot{\nu}$, as well as for 1337 ordinary isolated pulsars taken from ATNF database. The correlation coefficient between logarithms of these quantities is $r = 0.99$. The spread of points on the scatter plot is due to the distribution of frequencies ν among the pulsars. It, however, is unable to break tight relation between τ_{ch} and $\dot{\nu}$. Therefore, the frequency first derivative may also be considered a characteristic of pulsar age. Additionally, the obtained dependency $-\dot{\nu} \propto \tau_{ch}^\alpha$ with $\alpha \neq -1$ suggests the presence of significant $\dot{\nu} - \nu$ correlation (see Fig. 4)

while its $\dot{\nu}$ value increases and ν value decreases. However, on the negative branch of $\ddot{\nu} - \dot{\nu}$, the value of the first derivative, being negative too, can only decrease with time, since $\ddot{\nu}$ is a formal derivative of $\dot{\nu}$, and both of them are regular components of the observed rotational phase (1). So, pulsar motion along the branch may only be backward, which clearly contradicts its evolutionary interpretation suggested earlier. The solution we offer is to assume a *cyclic* behaviour of pulsars on this diagram. As pulsars evolve, they repeatedly change sign of $\ddot{\nu}$, in a spiral-like motion from branch to branch, and spend roughly half their lifetime on each one. Such behaviour is sketched in Figure 2.

The timescale of such variations has to be much shorter than the pulsar life time, and at the same time significantly larger than the one of the observations to systematically affect the timing solution. Of course, such cyclic behaviour should also affect other spin-down parameters – ν and $\dot{\nu}$.

Then, on $\dot{\nu} - \nu$ plot, shown in Figure 4, pulsars move from bottom right to the upper left, from high to low ν and $|\dot{\nu}|$, forming quasi-evolutionary sequence, with linear regression coefficient ~ 2 in logarithmic scale. Unfortunately, this diagram itself can’t be used to study the spin-down evolution of pulsars, as it is distorted by various selection effects (death line crossing, emission beam width dependency on pulsar frequency (Tauris & Manchester 1998), etc) and correlation of pulsars’ initial ν and $\dot{\nu}$ at birth.

3.2 Phenomenology of observed pulsars’ spin-down

Now we introduce an appropriate phenomenological description of the complex timing evolution of pulsars including the cyclic variations we proposed above.

The exact form of a pulsar’s trajectory on the $\ddot{\nu} - \dot{\nu}$ diagram is unknown, but in general its rotational evolution may

³ <http://www.atnf.csiro.au/research/pulsar/psrcat/>, revision from 6th Oct 2007

⁴ Data on PSR-SNR associations was also taken from ATNF.

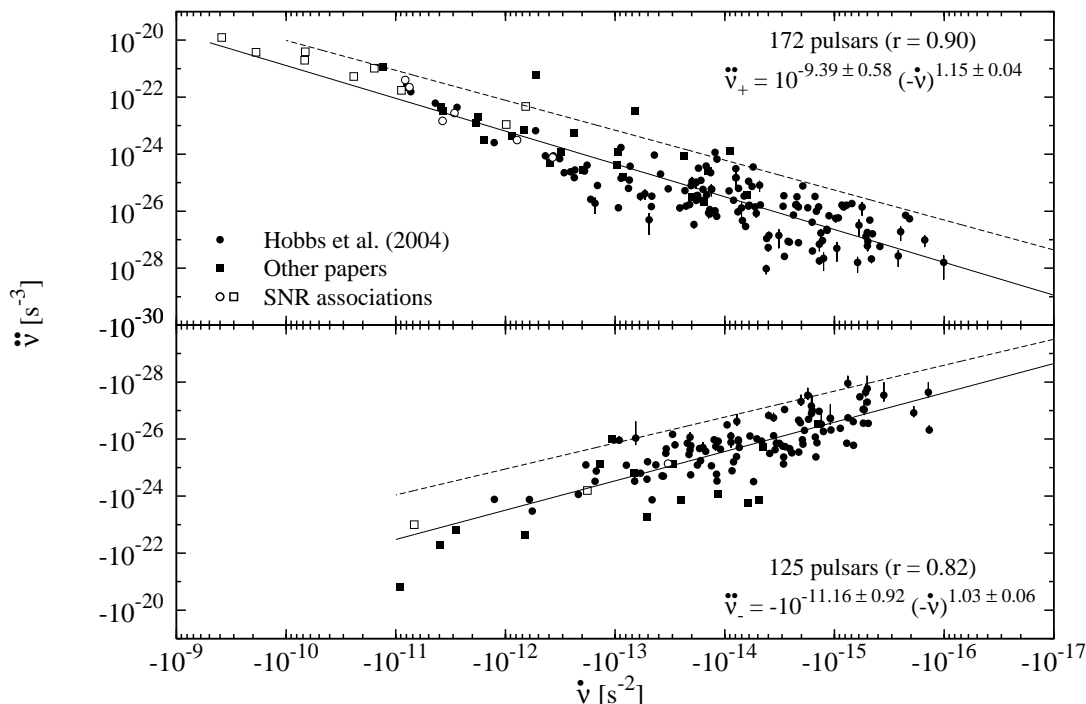


Figure 1. The $\ddot{\nu} - \dot{\nu}$ diagram for 297 pulsars. The figure shows the pulsars taken from Hobbs et al. (2004) as circles, and the objects measured by other groups as squares. Open symbols represent relatively young pulsars confidently associated with supernova remnants. Analytical fits for both positive and negative branches are shown as solid lines. They were obtained by means of linear least-squares regression in the logarithmic scale. Measurement errors are shown as error bars and in most cases are well inside the symbols. The diagram is an evolutionary sequence – pulsars systematically move from left to right of it. Two branches are due to cyclic variations of pulsars’ rotational parameters on a timescale significantly shorter than lifetime but longer than time spans of observations (Biryukov et al. 2007) as illustrated in Figure 2. The dashed lines represent the power-law approximations of the upper envelopes of positive and negative branches, estimated by the method described in (Cardiel 2009). Their moduli may be used as an upper and lower limits on the variational amplitude of $\ddot{\nu}$, respectively (see Section 3.4).

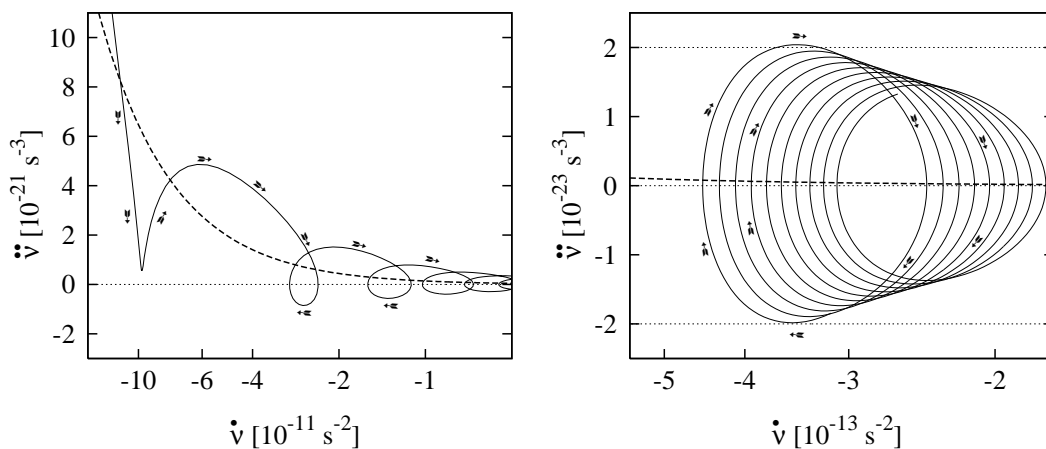


Figure 2. Concept illustration of a pulsar motion on the $\ddot{\nu} - \dot{\nu}$ diagram due to a cyclic evolution of the timing parameters. Monotonous component of a spin-down (dashed line) is according to a canonical law $\dot{\nu}_{ev} = -K\nu_{ev}^3$ with $K = 10^{-12} \text{ s}^2$ and $\nu_{ev}(0) = 30 \text{ Hz}$. Superimposed cyclic spin-down component is of a $\delta\dot{\nu}(t) = \dot{\nu}_{ev}(t)A \cos(\Omega t)$ form, with $A = 0.2$ and $2\pi/\Omega = 10^3$ years. Resultant track of a pulsar is shown as the solid line. On the *left* panel, an initial stages of pulsar evolution are presented – the track is shown for $10^{10} - 10^{11} \text{ s}$ interval of ages. Here the amplitude of $\ddot{\nu}$ variations is not much different from evolutionary value $\dot{\nu}_{ev}$, and therefore the youngest pulsars are unable to change the sign of their observed $\ddot{\nu}$. On the *right* panel the evolution of the same pulsar during $(1 - 1.3) \times 10^{12} \text{ s}$ ages interval is shown. Here, $\ddot{\nu}$ variations prevail, and the pulsar repeatedly changes the sign of $\ddot{\nu}$. Note, that due to positive contribution of $\dot{\nu}_{ev}$, variations are never exactly symmetric in respect to $\ddot{\nu} = 0$.

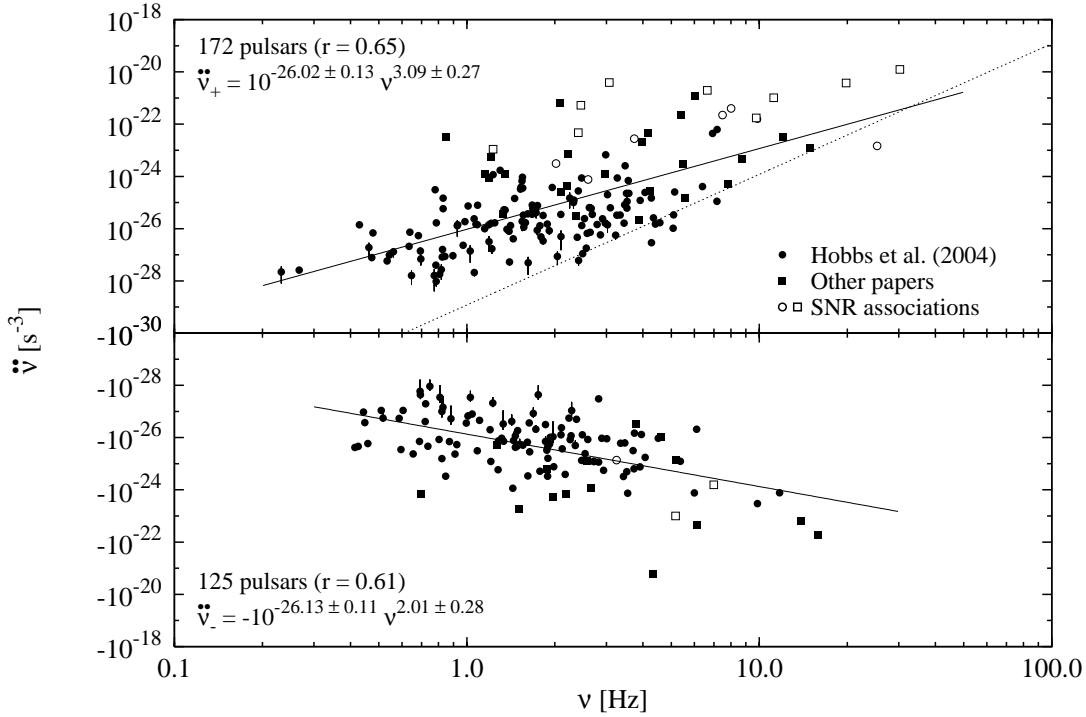


Figure 3. $\ddot{\nu} - \nu$ diagram for the subset of pulsars under investigation. This diagram is generally similar to the $\ddot{\nu} - \nu$ diagram shown in Fig. 1 and has the same evolutionary meaning, as pulsars born with higher values of ν and evolve to the lower ones. Dotted line shows typical evolutionary trend for a pulsar evolving according to $\dot{\nu} = -K\nu^n$ law with $K = 2 \times 10^{-15}$ and $n = 3$.

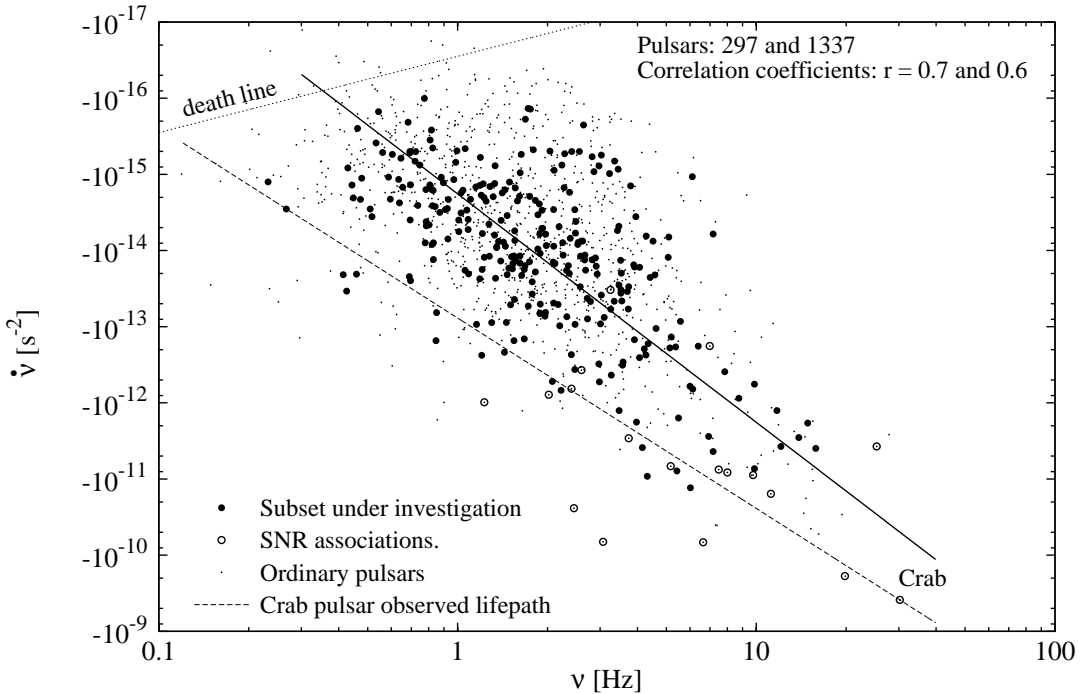


Figure 4. $\dot{\nu} - \nu$ diagram for 297 pulsars under investigation (circles) and 1337 “ordinary” isolated radiopulsars from ATNF database that satisfy the criteria from Sec. 2.2 excluding $\ddot{\nu}$ measurements. Extrapolation of present Crab pulsar motion assuming simple power-law spin-down with $n = 2.5$ is shown as dashed line. Also, the solid line shows a similar power-law trend for a typical pulsar with parameters derived through maximum likelihood estimator (Sec. 4) – i.e. with $n = 3$ and $K = \bar{K}(n = 3, \langle A \rangle = 0.65, \sigma[A] = 0.1)$. The pulsars’ death line $\dot{\nu} = -2.82 \times 10^{-17} \nu^{-1}$ is also shown according to (Bhattacharya et al. 1992)

be described as the superposition of the regular component of the observed rotational phase $\phi_{ev}(t)$, and an irregular, *cyclic* one $\delta\phi(t)$:

$$\phi(t) = \phi_{ev}(t) + \delta\phi(t), \quad (5)$$

where

$$\int_{\Delta T} \delta\phi(t) dt \approx 0 \quad (6)$$

over a long enough time interval ΔT comparable to a pulsar's lifetime. After term by term differentiation of equation (5) one gets:

$$\nu(t) = \nu_{ev}(t) + \delta\nu(t) \quad (7)$$

for the rotational frequency and

$$\dot{\nu}(t) = \dot{\nu}_{ev}(t) + \delta\dot{\nu}(t) = \dot{\nu}_{ev}(t) [1 + \varepsilon(t)] \quad (8)$$

for the spin-down rate $\dot{\nu}$. Obviously, due to secular loss of rotational energy, the value of $\dot{\nu}_{ev}(t)$ should be always negative for an isolated pulsar. Quantity $\varepsilon(t) \equiv \delta\dot{\nu}(t)/\dot{\nu}_{ev}(t)$ is a spin-down rate relative deviation, which is not necessarily small, and is likely greater than -1:

$$\varepsilon(t) > -1 \quad (9)$$

due to the absence of "ordinary" pulsars with $\dot{\nu} > 0$ in the subset under investigation. It is clear that deviation $\varepsilon(t)$ is also cyclic; in the simplest case it is a harmonic function of variational phase $\varphi(t)$:

$$\varepsilon(t) = A \cos \varphi(t), \quad (10)$$

where $\varphi(t) \equiv \varphi_0 + \Omega t$ and A is the relative amplitude of the $\dot{\nu}$ oscillations, related to the absolute amplitude $\mathcal{A}_{\dot{\nu}}$:

$$\mathcal{A}_{\dot{\nu}}(t) \equiv A \dot{\nu}_{ev}(t) \quad (11)$$

By second differentiation of equation (5) for a rotational frequency second derivative we get:

$$\ddot{\nu}(t) = \ddot{\nu}_{ev}(t) + \delta\ddot{\nu}(t) = \ddot{\nu}_{ev}(t) [1 + \eta(t)] \quad (12)$$

where $|\delta\ddot{\nu}(t)| \gg \ddot{\nu}_{ev}(t)$ (i.e. $|\eta(t)| \gg 1$) for most pulsars, and this is the reason behind anomalously high values of observed $|\ddot{\nu}|$ and braking indices. In other words, the absolute amplitude of the $\ddot{\nu}$ variations $\mathcal{A}_{\ddot{\nu}}$ is much greater than the regular term $\ddot{\nu}_{ev}$. Note also that cyclic terms $\varepsilon(t)$ and $\eta(t)$ are not independent – they are connected through the relation:

$$\eta(t) = \varepsilon(t) + \dot{\varepsilon}(t) \frac{\dot{\nu}_{ev}(t)}{\ddot{\nu}_{ev}(t)} \quad (13)$$

Since pulsars secularly evolve to the higher values of $\dot{\nu}$ and $\dot{\nu}_{ev}(t) < 0$, the sign of $\ddot{\nu}_{ev}(t) = d\dot{\nu}_{ev}(t)/dt$ should always be positive:

$$\ddot{\nu}_{ev}(t) > 0 \quad (14)$$

Such positive contribution should introduce a small asymmetry of the observed values of $\ddot{\nu}$ in respect to $\ddot{\nu} = 0$, even if the variations of $\delta\ddot{\nu}$ are intrinsically symmetric. Such asymmetry drives the average motion to the right on the $\ddot{\nu} - \dot{\nu}$ diagram and affects the times that pulsars spend with positive and negative $\ddot{\nu}$.

3.3 Asymmetry in observed $\ddot{\nu}$'s

Indeed, numbers of pulsars with positive ($N^+ = 172$) and negative ($N^- = 125$) values of $\ddot{\nu}$ within the subset are significantly different. If this difference is just accidental, its probability is too small, $P = 6.4 \times 10^{-3}$ only, assuming binomial distribution of 297 objects with $p = 1/2$ chance to be on a positive branch. Therefore, null hypothesis of exactly symmetric branches is rejected on a 0.64% significance level, and the branches are indeed asymmetric in number of objects⁵.

We investigated in detail the behaviour of such significance levels for a number of subsets of pulsars with $\dot{\nu}$ greater than and ν less than a given value. Corresponding dependencies are plotted in the Fig. 6. It is clearly seen that branches of the $\ddot{\nu} - \dot{\nu}$ and $\ddot{\nu} - \nu$ diagrams are significantly different only when relatively young pulsars are taken into account, while behaviour of the older pulsars seems to be the same for both signs of $\ddot{\nu}$. It is consistent with the existence of a positive evolutionary trend $\ddot{\nu}_{ev}$, which is negligible for older pulsars, but is large enough to affect the second derivatives of the younger ones.

In other words, for the initial stages of pulsars life, values of $|\delta\ddot{\nu}|$ are less than $\ddot{\nu}_{ev}$ (i.e. $|\eta(t)| < 1$), and the second derivatives are always positive (see the upper left region of Fig. 1). Later on, as $|\dot{\nu}|$ decreases, the $\ddot{\nu}_{ev}$ becomes quite small and the relative deviations $|\eta(t)|$ grow up extremely over unity; as a result, observed values of $\ddot{\nu}$ turn out to be significantly different from an intrinsic $\ddot{\nu}_{ev}$, and it corresponds to the great increase of their absolute braking indices (see Fig. 7). These different stages of pulsars' evolution are illustrated in the Fig. 2.

At the same time, the absence of a significant difference between the $\ddot{\nu} - \dot{\nu}$ branches for relatively old pulsars – their symmetry – implies an important fact that $\delta\ddot{\nu}$ variations are indeed approximately symmetric in respect to evolutionary trend: a pulsar deviates to higher and lower values of $\ddot{\nu}$ with nearly the same amplitude and spends an equal amounts of time with $\ddot{\nu}$ greater and less than $\ddot{\nu}_{ev}$. This fact will be used in Section 4 for the estimation of the parameters of pulsars' two-component spin-down model.

However, some generic characteristics of the cyclic, irregular component of $\ddot{\nu}$ behaviour – its amplitude and timescale – may be easily derived from an exploratory analysis of the $\ddot{\nu} - \dot{\nu}$ and $n_{obs} - \tau_{ch}$ scatter plots using simple, model-independent arguments. Such analysis is presented in the next two subsections.

3.4 Simple limits on the timescales and amplitudes of the cyclic process

As stated above, for the majority of pulsars the amplitude $\mathcal{A}_{\ddot{\nu}}$ of the second derivative variations is much greater than the positive evolutionary trend $\ddot{\nu}_{ev}$. All the pulsars on the negative branch of $\ddot{\nu} - \dot{\nu}$ diagram are due to subtraction of this amplitude from the trend. Therefore, the values of $|\ddot{\nu}|$ of the lower envelope of this branch (in terms of $|\ddot{\nu}|$) are sensible estimation of a *lower* limit on $\mathcal{A}_{\ddot{\nu}}$. At the same time,

⁵ At the same time, non-parametric Kolmogorov-Smirnov test rejects the hypothesis of the common distribution of $|\ddot{\nu}|$ of positive and negative branches on a 2.5% significance level.

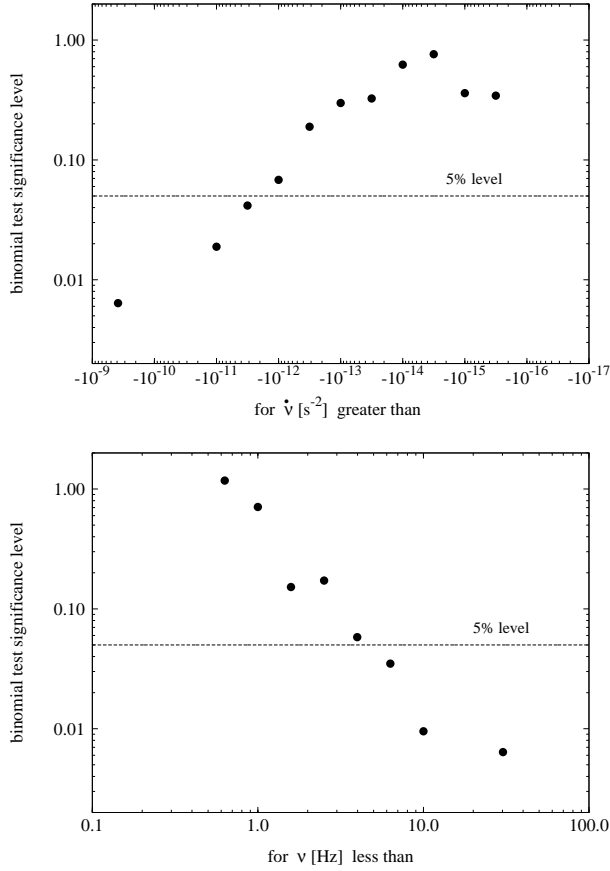


Figure 6. The significance levels of a non-parametric binomial test for the hypothesis of equal numbers of pulsars with $\ddot{\nu} > 0$ and $\ddot{\nu} < 0$. Each point on the plots represents the p -values for the subset of pulsars with $\dot{\nu}$ greater than (upper) and ν less than (bottom) selected threshold. Minimal significance levels correspond to the complete set of pulsar. So, the differences of branches in number of pulsars are due to contribution of the youngest objects. The absence of any significant branch differences for older pulsars favors the assumption of symmetric variations of $\ddot{\nu}$ in respect to its evolutionary values.

the values of $\ddot{\nu}$ of pulsars near upper envelope of positive branch may be considered an *upper* limit of $\mathcal{A}_{\ddot{\nu}}$.

Indeed, due to existence of the secular trend $\ddot{\nu}_{ev} > 0$, the amplitude of the variational term $\delta\ddot{\nu}$ can not exceed the values of $\ddot{\nu}$'s of the upper envelope of the positive branch (for a given $\dot{\nu}$). For pulsars there $\ddot{\nu} = \ddot{\nu}_{ev} + \delta\ddot{\nu} = \ddot{\nu}_{ev} + \mathcal{A}_{\ddot{\nu}} > \mathcal{A}_{\ddot{\nu}}$, while for ones on the lower envelope of the negative branch $|\ddot{\nu}| < \mathcal{A}_{\ddot{\nu}} - \ddot{\nu}_{ev} < \mathcal{A}_{\ddot{\nu}}$.

We used the **BoundFit** generalized least-squares code developed by Cardiel (2009) to acquire an analytical expressions for the mentioned envelopes of the negative and positive branches on the $\ddot{\nu} - \dot{\nu}$ diagram, and found them to be

$$\mathcal{A}_{\ddot{\nu},low} = 10^{-14.03}(-\dot{\nu})^{0.91} \approx 10^{-14.03}(-\dot{\nu}_{ev})^{0.91} \quad (15)$$

and

$$\mathcal{A}_{\ddot{\nu},up} = 10^{-9.51}(-\dot{\nu})^{1.05} \approx 10^{-9.51}(-\dot{\nu}_{ev})^{1.05} \quad (16)$$

respectively. They are shown as dashed lines in Figure 1.

Since we consider pulsars on fits (15) and (16) to be ob-

served with amplitude values of frequency second derivative, their $\ddot{\nu}$'s are close to turning points, where corresponding $\delta\dot{\nu}$ change signs during the oscillations (see also the sketch in Figure 2), and are obviously small ($\delta\dot{\nu} \approx 0$). Hence, the assumption of $\dot{\nu} \approx \dot{\nu}_{ev}$ in equations (15) and (16) is justified.

Due to the absence of pulsars with positive $\dot{\nu}$, the amplitudes of variations of frequency first derivatives are likely to be less than their secular values: $\mathcal{A}_{\dot{\nu}} < -\dot{\nu}_{ev}$ and $\mathcal{A}_{\dot{\nu},up} \sim -\dot{\nu}_{ev}$. Also, for any more or less stable cyclic process, the following relations should be true:

$$\Omega \sim \frac{\mathcal{A}_{\ddot{\nu}}}{\mathcal{A}_{\dot{\nu}}} \sim \frac{\mathcal{A}_{\ddot{\nu}}}{\mathcal{A}_{\dot{\nu}}}, \quad (17)$$

where $\Omega = 2\pi/T$ is a characteristic frequency of cyclic variations. (For the special case (10) these relations are exact). For the upper limit $\Omega_{up} \sim \mathcal{A}_{\ddot{\nu},up}/\mathcal{A}_{\dot{\nu},low}$ while for the lower one $\Omega_{low} \sim \mathcal{A}_{\ddot{\nu},low}/\mathcal{A}_{\dot{\nu},up}$. Hence, one can estimate:

$$T_{up} = \frac{2\pi}{\Omega_{low}} < -2\pi \frac{\dot{\nu}_{ev}}{\mathcal{A}_{\ddot{\nu},low}}, \quad (18)$$

which leads to upper limit on the timescale T_{up} :

$$T_{up} \sim (1.2 \times 10^6 \text{ years}) \cdot (-\dot{\nu}_{ev,14})^{0.09}, \quad (19)$$

where $\dot{\nu}_{ev}$ is normalized to 10^{-14} s^{-2} . The value of T_{up} changes from $\approx 8 \times 10^5$ years for oldest to $\approx 2 \times 10^6$ years for youngest pulsars. Then, the value of lower limit T_{low} should depend on the upper limit of $\mathcal{A}_{\ddot{\nu}}$ and typical minimal relative $\delta\dot{\nu}$ amplitude A_m : $\mathcal{A}_{\dot{\nu},low} = -A_m\dot{\nu}_{ev}$. Hence

$$T_{low} \sim -2\pi \frac{\mathcal{A}_{\ddot{\nu},up}}{\mathcal{A}_{\dot{\nu},up}} \quad (20)$$

or

$$T_{low} \sim (650 \text{ years}) \cdot A_m \cdot (-\dot{\nu}_{ev,14})^{-0.05} \quad (21)$$

However, T should be more than few times of typical observational span length for the pulsars under investigation, which is 15 – 20 years. Hence,

$$T_{low} \sim 50 - 100 \text{ years} \quad (22)$$

and A_m is unlikely less than ~ 0.1 . Moreover, we will show below that A_m is even greater than ~ 0.5 .

At the same time, assuming that fit to negative branch of $\ddot{\nu} - \dot{\nu}$ diagram

$$\ddot{\nu}_- = -10^{-11.16} \cdot (-\dot{\nu})^{1.03} \approx -10^{-11.16} \cdot (-\dot{\nu}_{ev})^{1.03} \quad (23)$$

represents in the same way a *typical* variational amplitude (shown as solid line $\ddot{\nu}_-(\dot{\nu})$ in Figure 1), one may, in a similar way, estimate a typical timescale able to provide observed $\ddot{\nu}$ spread. So, $\Omega_{typ} = |\ddot{\nu}_-|/\dot{\nu}_{ev}$ or

$$T_{typ} = \frac{2\pi}{\Omega_{typ}} = (7.5 \times 10^4 \text{ years}) \cdot (-\dot{\nu}_{ev,14})^{0.03} \quad (24)$$

with spread from $\sim 6 \times 10^4$ to $\sim 9 \times 10^4$ years for oldest and youngest objects, respectively.

Finally, according to equation (17) the amplitudes of the pulsars' frequency variations should be roughly Ω^{-1} times the ones of its derivative and Ω^{-2} times – its second one. For typical maximal timescale (24):

$$\mathcal{A}_{\dot{\nu}} < \dot{\nu}_{ev}^2/|\ddot{\nu}_-| = (4 \times 10^{-3} \text{ Hz}) \cdot (-\dot{\nu}_{ev,14})^{0.97} \quad (25)$$

These values do not exceed a few Hertz even for young pulsars and significantly less than observed frequencies for most

of pulsars. It justifies the neglect of variational term in the rotational frequency decomposition (7):

$$\delta\nu(t) < \nu_{ev}(t) \text{ and } \nu(t) \approx \nu_{ev}(t) \quad (26)$$

3.5 Pulsar observed braking indices and characteristic ages. An analysis of the $n_{obs} - \tau_{ch}$ diagram.

There are number of widely accepted estimators of pulsars' physical properties based on results of timing solution and power-law (3) spin-down model with constant K and $n = 3$: characteristic age $\tau_{ch} = -\nu/2\dot{\nu}$, rotational energy loss rate $\dot{E}_{rot} \propto \nu\dot{\nu}$ and surface magnetic field

$$B = (3.2 \times 10^{19} \text{ G}) \sqrt{-\dot{\nu}\nu^{-3}}. \quad (27)$$

But, if the amplitude of frequency derivative variations, $|\varepsilon(t)|$, is large, these quantities may be significantly biased, as they are computed using observed $\dot{\nu}$ values, and not actual evolutionary ones $\dot{\nu}_{ev}$.

Using phenomenology introduced earlier and assuming power-law spin-down defined by equation (3) with constant K and evolutionary braking index n , observed quantities n_{obs} and τ_{ch} may be expressed as:

$$n_{obs} = n \frac{1 + \eta}{(1 + \varepsilon)^2} \quad (28)$$

and

$$\tau_{ch} = \left(\frac{n-1}{2}t + \frac{P_0^{n-1}}{2K} \right) \frac{1}{1+\varepsilon} = \frac{\tau_{ch,ev}}{1+\varepsilon}, \quad (29)$$

where P_0 is pulsar initial period, t – its real age, and ε and η are relative $\dot{\nu}$ and $\ddot{\nu}$ deviations according to equations (8) and (12). If $n = 3$, then $P_0^2/2K \sim 10^3$ years for the typical pulsar and $\tau_{ch,ev} \approx t$ for the older objects.

So, if ε varies in ± 0.9 range, then half of pulsars will be observed as up to $\tau_{ch}/\tau_{ch,ev} \approx 1/(1-0.9) = 10$ times older than their true unbiased characteristic ages, while another half as $1/(1+0.9) \approx 0.5$ times younger. The effect is therefore seemingly asymmetric, as characteristic ages will mostly appear overestimated.

The same bias will also appear in the rotational energy loss rate, while magnetic fields will be 2 – 3 times underestimated for pulsars with $\varepsilon < 0$.

Moreover, since observed braking indices $n_{obs} = \nu\ddot{\nu}\nu^{-2} \propto \dot{\nu}^{-2}$, their absolute values will be additionally increased up to order of magnitude for a half of pulsars.

Since n_{obs} and τ_{ch} depend on $\varepsilon(t)$ and $\eta(t)$, the pulsar behaviour on the $n_{obs} - \tau_{ch}$ plane, shown in Figure 7, is similar to that in the $\ddot{\nu} - \dot{\nu}$ one. The positive and negative branches are not identical: the numbers of pulsars and shapes of branches are significantly different.

The most interesting regions of the diagram are the areas I, II and III with the relatively young pulsars. There are 19 pulsars with positive and only 2 with negative n_{obs} in the area III⁶. Binomial test with $p = 1/2$ rejects the hypothesis

of an accidental origin of such asymmetry on a 0.01% significance level. The pulsars with positive n_{obs} have measured $n_{obs} \sim 10 - 50$, which are larger than any reasonable secular value. Moreover, they slightly deviate from the rest of positive branch of the diagram.

Is it possible to explain these n_{obs} as a result of decay of K coefficient in spin-down law (3), probably due to evolution of magnetic inclination angle (e.g. Davis & Goldstein (1970))? To yield pulsars with both $n_{obs} \sim 30 - 50$ and $\tau_{ch} \sim 10^4$ years, corresponding timescale $-K/\dot{K}$ should be as short as few thousands years only. However, e.g. Faucher-Giguère & Kaspi (2006) have shown that there is no significant decay of coefficient K on a timescale $\sim 10^8$ years for isolated pulsars.

We plotted pulsar evolutionary tracks corresponding to spin-down law (3) with $n = 3$ and $-K/\dot{K} = 5 \times 10^4$ and 10^7 years on the $n_{obs} - \tau_{ch}$ diagram (blue dashed lines in Figure 7). It is clearly seen that first of them is insufficient to explain n_{obs} of pulsars in area III, while second one is unable to affect observed distribution of pulsars' n_{obs} at all.

So, we conclude that such asymmetry results from combination of a small enough amplitudes of $\dot{\nu}$ variations (i.e. $|\eta| \ll 1$, so the negative values of $\dot{\nu}$ can not be reached yet) and high amplitudes of $\dot{\nu}$ ones. Assuming $n = 3 - 5$ and $\eta = 0$, for these pulsars with $n_{obs} = 50$ from relation (28) one get:

$$\varepsilon \approx \sqrt{\frac{n}{n_{obs}}} - 1 = -0.76 - -0.68 \quad (30)$$

Therefore, the existence of such a remarkable group of pulsars on the $n_{obs} - \tau_{ch}$ diagram argues in favour of significantly high relative amplitudes of $\dot{\nu}$ variations – $\delta\dot{\nu}(t)$ in decomposition (8).

Young pulsars in the area III are mostly the ones with negative ε . Since the variational process is likely symmetric relative to evolutionary trend $\dot{\nu}_{ev}$, young pulsars with positive values of ε should exist with $\tau_{ch} < \tau_{ch,ev}$ and n_{obs} that is likely less than n .

The pulsars of area I seem to be exactly such objects. They all have $n_{obs} < 3$ and their observed characteristic ages are most likely shifted towards lower values. Also, there is a deficit of pulsars in the area II⁷ (with $\tau_{ch} = 2 - 7$ kyr) which may be a result of pulsars escaping from there to lower and higher τ_{ch} due to positive and negative ε , correspondingly. So, the variations can be a reason for $n_{obs} < 3$ measured for the youngest pulsars known. We will return to the analysis of the youngest pulsars within our concept of cyclic variations in the Discussion.

Finally, all remaining pulsars on the diagram – objects of the area IV – form two nearly symmetric branches with positive and negative n_{obs} . The variational amplitudes of $\dot{\nu}$ of these pulsars are much larger than corresponding evolutionary values: $|\eta| \gg 1$. They are also affected by large amplitudes of $\dot{\nu}$ variations that may produce the oldest (with $\tau_{ch} > 10^7 - 10^8$ years) observed pulsars. Indeed, the largest pulsars' τ_{ch} seem to be physically unreasonable, as pulsars

⁶ Moreover, these two pulsars with negative $\dot{\nu}$ (PSR B1338-62 and PSR B1610-50), while satisfying to the formal selection criteria described in Sec. 2.2, have relatively bad data sets – B1338-62 shows significant glitch activity, and time spans for both of them are only about 200 days long.

⁷ Note, however, that at least six “ordinary” pulsars without $\ddot{\nu}$ measurement are known in this area. Their ages concentrate near $\tau_{ch} \sim 3$ and 5 kyr as seen from the set of red vertical strokes in Figure 7

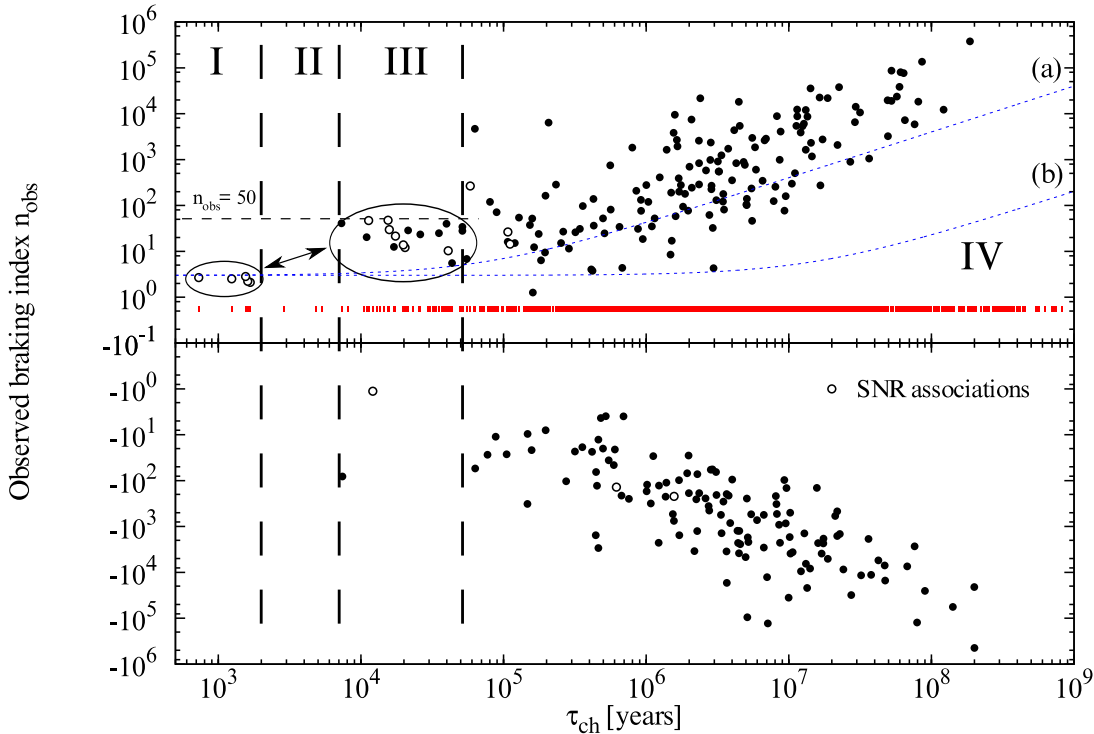


Figure 7. The $n_{obs} - \tau_{ch}$ diagram. It is similar to the $\ddot{\nu} - \dot{\nu}$ one shown in Figure 1. Correlation coefficients for positive and negative branches in logarithmic scale are 0.78 and 0.76 respectively. Red vertical strokes represent values of τ_{ch} of 1337 ordinary pulsars, displayed to show overall distribution of τ_{ch} . The younger pulsars, particularly associated with SNRs, are located on the left part of the diagram (areas I, II and III). Their $\dot{\nu}$ amplitudes are still quite small and are unable to produce negative observed n_{obs} even in area III. However, the braking indices of pulsars there are obviously anomalous ($n_{obs} \lesssim 50$), and can not be explained by non-constant coefficient in spin-down law (3) as illustrated by blue dashed lines representing pulsar tracks with $-K/\dot{K} = 5 \times 10^4$ (a) and 10^7 (b) years, respectively. It suggests that these values are primarily affected by large $\dot{\nu}$ variations ($A \sim 0.5 - 0.7$). At the same time, the lack of objects in area II combined with small n_{obs} of pulsars of area I means that observed braking indices and ages of the latter group are likely to be also affected by $\dot{\nu}$ variations. The observed τ_{ch} of the youngest pulsars seem to be less than evolutionary values, while τ_{ch} of pulsars of area III *vice versa* are greater. The amplitudes of $\dot{\nu}$ variations of pulsars of area IV are much greater than evolutionary values which produces two nearly symmetric branches of the diagram.

should cross their “death lines” in a few millions of years only (Bhattacharya et al. 1992; Faucher-Giguère & Kaspi 2006).

4 PULSARS’ SPIN-DOWN MODEL

In the previous section we performed a statistical analysis of pulsars rotational parameters and concluded that observed pulsar spin-down is consistent with an idea of the existence of some cyclic variational process. Model-independent estimations show that this process operates on timescales as long as few hundreds or thousands of years, while relative amplitudes of $\dot{\nu}$ variations are comparable to secular, monotonous component of pulsar spin-down $\dot{\nu}_{ev}$.

Also, we found some evidence that $\ddot{\nu}$ variations are symmetric in respect to evolutionary term $\dot{\nu}_{ev}$. This fact may be useful to reveal the parameters of the evolutionary component, common for all pulsars.

In the Section below we construct a two-component model of observed pulsars’ rotational evolution which consists of evolutionary monotonous and cyclic components according to decomposition (8), and derive its parameters.

4.1 Monotonous component of observed spin-down

For the secular spin-down term of our model we will assume canonical power-law expression:

$$\dot{\nu}_{ev} = -K\nu_{ev}^n, \quad (31)$$

with $K = const$ unique for each pulsar. On the other hand, we presume the constant *evolutionary* braking index n to be the same for all pulsars. The observed quantity n_{obs} and model parameter n are not equivalent and are connected with relation (28) for each pulsar.

Combining equations (7), (8) and (31), the evolutionary value of second frequency derivative for each pulsar with observed ν and $\dot{\nu}$ may be written either as

$$\ddot{\nu}_{ev,1} = nK^2\nu^{2n-1} \quad (32)$$

or as

$$\ddot{\nu}_{ev,2} = nK^{\frac{1}{n}} \left(-\frac{\dot{\nu}}{1+\varepsilon} \right)^{2-\frac{1}{n}} \quad (33)$$

These expressions correspond to projections of an evolutionary trend onto either $\ddot{\nu} - \nu$ or $\ddot{\nu} - \dot{\nu}$ planes, respectively.

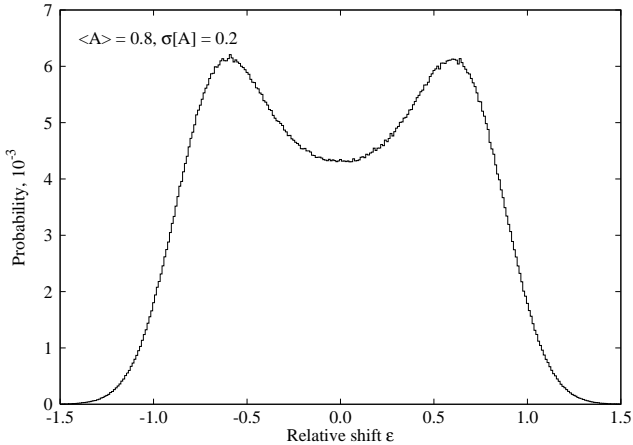


Figure 8. Distribution of relative deviations ε simulated according to relation (34) and distributions (35) and (36) with $\langle A \rangle = 0.8$ and $\sigma[A] = 0.2$. The probability $P(\varepsilon < -1)$ determines the probability for pulsar to be observed with positive $\dot{\nu}$.

Moreover, when computed using actually measured timing parameters, these quantities may be treated as a statistically independent ones, as they arise from combinations of different observables.

4.2 Cyclic term of observed spin-down

As a toy model, not necessarily exact but still representing all the important properties, we assume below a simple harmonic form for an oscillating term of sum (8):

$$\varepsilon(t) = A \cos \varphi(t), \quad (34)$$

where A is a constant relative amplitude, and $\varphi(t)$ is a phase of variations.

Actual values of ε for individual pulsars, as well as values of coefficient K in the law (31), are unknown. Therefore, we will analyse our subset in terms of its average, ensemble characteristics only. The parameters of ε 's distribution will be included in the model.

Namely, to take into account physical diversity of individual pulsars, we assume A to be normally distributed with mean $\langle A \rangle$ and variance $\sigma^2[A]$:

$$A \sim \mathcal{N}(\langle A \rangle, \sigma^2[A]). \quad (35)$$

At the same time, the phase φ is obviously distributed uniformly,

$$\varphi \sim \text{Uni}(0, 2\pi), \quad (36)$$

as it depends (as a modulus of $\varphi = \varphi_0 + f(T, t)$ quantity over 2π) both on an unknown value of initial phase φ_0 and randomly selected moment of observations – pulsar' age t . It is also safe to assume the phases of individual pulsars to be uncorrelated both over the ensemble and with pulsar' parameters.

Simulated ε distribution for typical parameters of $\langle A \rangle = 0.8$ and $\sigma[A] = 0.2$ is shown in Figure 8. Values of ε less than -1 correspond to the positive observed $\dot{\nu}$ since $\dot{\nu} = \dot{\nu}_{ev}(1 + \varepsilon)$. The probability to find a pulsar with $\dot{\nu} > 0$:

$$P_{pos} \equiv \mathcal{P}(\varepsilon < -1) \quad (37)$$

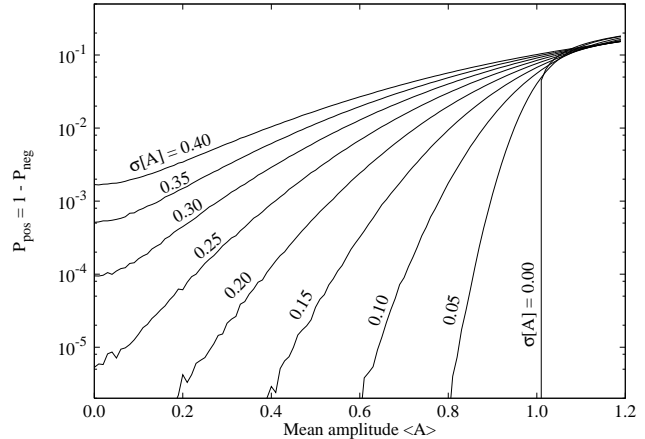


Figure 9. Probability $P_{pos} \equiv \mathcal{P}(\varepsilon < -1)$ for a pulsar to be observed with positive $\dot{\nu}$ for different combinations of parameters $\langle A \rangle$ and $\sigma[A]$ of ε distribution.

for such a model depends on the parameters of the ε distribution $\langle A \rangle$ and $\sigma[A]$. This dependence is shown in Figure 9.

4.3 Evolution of an ensemble of pulsars

Since we assume n to be the same for all pulsars, their trends $\dot{\nu}_{ev}(\nu_{ev})$ on the $\dot{\nu} - \nu$ diagram are characterized by individual coefficients K and initial frequencies ν_0 only. These trends are straight lines in logarithmic scale (see Figure 4) and do not intersect each other. Hence, the average behaviour of a pulsars' ensemble may be characterized by the line separating the set of their evolutionary trajectories in half. Such trend corresponds to the median value of the coefficient $K = -\dot{\nu}_{ev}/\nu_{ev}^n$:

$$\hat{K} = \mathcal{M} \left[-\frac{\dot{\nu}}{\nu^n} \frac{1}{1 + \varepsilon} \right], \quad (38)$$

where $\mathcal{M}[\cdot]$ is a median over an ensemble and relations (8) and (26) are used. The value of $\hat{K} = \hat{K}(n)$ can not be estimated from observables only since values of ε for individual pulsars are unknown, but one can build a distribution of \hat{K} assuming statistical properties of ε within the ensemble. This distribution is a function of three parameters:

$$\hat{K} = \hat{K}(\langle A \rangle, \sigma[A], n) \quad (39)$$

It will be used below to build a maximum likelihood estimator for the parameters of the pulsars in the ensemble.

4.4 Criterion for the estimation of model parameters

If the $\dot{\nu}$ distribution is symmetric with respect to $\dot{\nu}_{ev}$, then the numbers of objects with observed $\dot{\nu}$ less and greater than corresponding $\dot{\nu}_{ev}$ should be nearly equal, both for the whole ensemble and for any subset defined by quantities uncorrelated with phase (i.e. ν or $\dot{\nu}$). It provides a simple criterion for a model goodness-of-fit for an appropriately chosen $\dot{\nu}_{ev,i}$ (defined by equations (32) and (33)) the numbers of pulsars observed with $\dot{\nu} > \dot{\nu}_{ev,i}$ should *simultaneously*, for both $i = 1, 2$ be distributed binomially as

$$N_i^+ \sim \text{Bin}(N, p = \frac{1}{2}), \quad (40)$$

where N is the total number of pulsars in the ensemble. The same should obviously be valid for any sub-interval along ν or $\dot{\nu}$: if the number of pulsars in k -th sub-interval on i -th plane is N_{ik} , then the probability to have N_{ik}^+ of N_{ik} pulsars with $\dot{\nu} > \dot{\nu}_{ev}$ is

$$P_{ik} = \frac{N_{ik}!}{(N_{ik} - N_{ik}^+)! \cdot N_{ik}^+!} \cdot \left(\frac{1}{2}\right)^{N_{ik}} \quad (41)$$

Using this criterion and the dependence of N_{ik}^+ on the parameters of pulsars' spin-down model, an obvious maximum likelihood estimator can be constructed to derive these parameters.

4.5 Maximum likelihood estimator for the model parameters

The estimation of N_{ik}^+ for any interval of ν or $\dot{\nu}$ requires exact values of $\dot{\nu}_{ev,i}$ and, hence, known specific K and ε for each pulsar. These values can not be derived directly from observational data and therefore we have to hypothesize about them.

We adopted the following routine for its estimation. Since no *ad hoc* information is available on ε , we assumed it to be a random value distributed according to equations (34)-(36). The specific K has been, in turn, replaced with median \hat{K} value computed according to relation (38) with these ε values in mind. This way, the corresponding estimates for the monotonous component of the second frequency derivatives for each pulsar from equations (32)-(33),

$$\hat{\nu}_{ev,1} = n\hat{K}^2\nu^{2n-1} \quad (42)$$

and

$$\hat{\nu}_{ev,2} = n\hat{K}^{\frac{1}{n}} \left(-\frac{\dot{\nu}}{1+\varepsilon}\right)^{2-\frac{1}{n}} \quad (43)$$

are in turn random quantities, uncorrelated to each other as they arise from combinations of different observables. They are, however, median estimates of its exact values due to functional form of equations, and therefore should roughly divide an ensemble of pulsars in half for adequately chosen model parameters – n , $\langle A \rangle$ and $\sigma[A]$.

So, to construct maximum likelihood estimator we divided all pulsars into $m = 6$ intervals of $N_{ik} \approx 50$ objects each ($k = 1, 2, \dots, m$) along ν and $\dot{\nu}$ on the $\dot{\nu} - \nu$ and $\dot{\nu} - \nu$ planes, respectively. Then we calculated a likelihood function as follows:

- On the first step specific values of $\langle A \rangle$, $\sigma[A]$ and n have been chosen from the parameter space.
- Then $N = 297$ values of ε have been simulated according to distributions (35) and (36), and
- $\hat{K}(n, \langle A \rangle, \sigma[A])$ have been determined.
- The number of pulsars N_{ik}^+ with $\dot{\nu} > \hat{\nu}_{ev,ik}$ in k^{th} interval have been calculated and
- used to compute binomial probabilities P_{ik} defined (41).
- Then, the likelihood functions has been constructed:

$$\ell_i = \prod_{k=1}^m P_{ik} \quad (44)$$

We have also taken into account an absence of pulsars with positive $\dot{\nu}$ in an ensemble of $N = 297$ pulsars. This fact

constraints the parameters of ε distribution, as probability P_{pos} for the pulsar to be observed with positive $\dot{\nu}$ unlikely exceeds $1/N$ and corresponding probability

$$P_{neg} = 1 - P_{pos} > 1 - \frac{1}{N} \quad (45)$$

for the pulsar to be observed with *negative* $\dot{\nu}$ therefore has to be large enough.

The binomial probability P_{neg}^N to observe all N pulsars with *negative* values of $\dot{\nu}$ has therefore been added as a multiplicative term to the likelihood function, and

- finally we calculated logarithmic likelihood functions as

$$\mathcal{L}_i = -N \log P_{neg} - \sum_{k=1}^m \log P_{ik} \quad (46)$$

The indices $i = 1$ and 2 here mark (statistically independent) likelihoods for the planes $\dot{\nu} - \nu$ and $\dot{\nu} - \dot{\nu}$, respectively.

We performed simulations of relative deviations $\varepsilon = \delta\dot{\nu}/\dot{\nu}$ for 297 pulsars 10^4 times in a row⁸ for each set of given $\langle A \rangle$, $\sigma[A]$ and n . In this way, the distributions (but not exact values) of \mathcal{L}_i for every combination of parameters have been obtained. We have computed these distributions over a grid of values n , $\langle A \rangle$ and $\sigma[A]$ in the intervals $0.5 - 6.5$, $0 - 1.2$ and $0 - 0.4$ with steps 0.05 , 0.01 and 0.05 , respectively.

4.6 Likelihood for the null hypothesis

Classical maximum likelihood technique presuppose a search of extremum of obtained \mathcal{L} within parameters space and then constraining the confidence regions assuming that distribution of \mathcal{L} is known if the null hypothesis is valid. Typically \mathcal{L} is a single-valued function of model parameters, and the p -% confidence region consists of a values of \mathcal{L} for that $P(\mathcal{L}_0 < \mathcal{L}) \leq p/100$, where \mathcal{L}_0 is a random quantity distributed as a logarithmic likelihood within null hypothesis. The minimum of \mathcal{L} is obviously within this confidence region.

This method may be generalized in a straightforward way for the case when \mathcal{L} is not a deterministic function of parameters but a random quantity with known distribution.

To do it, we simulated the distribution of \mathcal{L}_0 by computing its values in a way similar to one used earlier for \mathcal{L}_i , but using N_{ik}^+ *simulated* according to binomial distribution with $p = 1/2$, and *simulated* uniformly distributed P_{neg} on the $[(N-1)/N; 1]$ interval. Therefore, the null hypothesis corresponds to the exact symmetry of numbers of pulsars with $\dot{\nu}$ greater and less than $\hat{\nu}_{ev,i}$ in each of m intervals described above.

Then, using known distribution of \mathcal{L}_i , we independently estimated the probabilities $\mathcal{P}_i = P(\mathcal{L}_0 < \mathcal{L}_i)$ and conflated them into the resulting united value \mathcal{P} using the method described by Hill & Miller (2010) and Hill (2011):

$$\mathcal{P} = \frac{\mathcal{P}_1 \mathcal{P}_2}{\mathcal{P}_1 \mathcal{P}_2 + (1 - \mathcal{P}_1)(1 - \mathcal{P}_2)} \quad (47)$$

This relation represents the cumulative probability that both likelihood functions have an extremum in the same

⁸ All simulations have been performed using the ‘‘Chebyshev’’ supercomputer of Moscow State University.

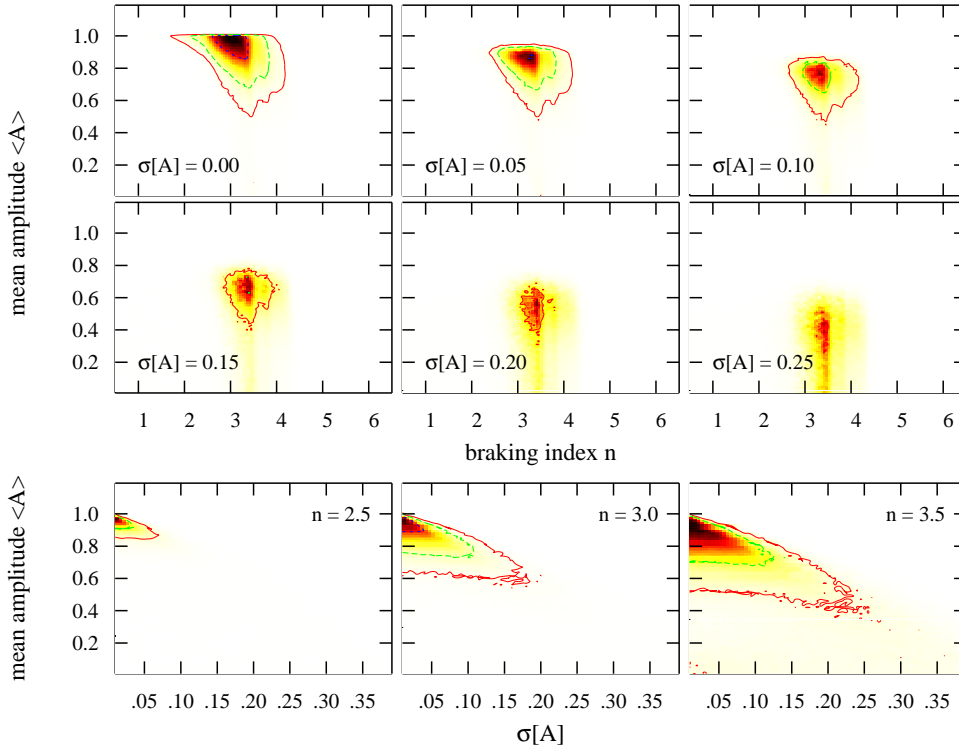


Figure 10. Plot of the confidence regions derived through the maximum likelihood estimator. The number of slices for fixed $\sigma[A]$ and n are shown. Blue, green and red contours represent 65, 95 and 99% bounds. The values of evolutionary braking index n , mean amplitude $\langle A \rangle$ and its dispersion $\sigma[A]$, consistent with the symmetry of $\dot{\nu}$ variations, are at $n \sim 2.5 - 4$, $\langle A \rangle > 0.5$ and $\sigma[A] < 0.25$.

point of a model parameters space. Thus, the isocontours of \mathcal{P} mark the bounds of a $100 \cdot (1 - \mathcal{P})$ percent confidence regions.

4.7 Results of maximum likelihood estimation

The maps of final conflated probabilities P are shown in the Fig. 10 as a collection of slices of the parameter space for fixed $\sigma[A]$ (upper plots) or n (lower plots). The 99% confidence interval covers the range of n :

$$2.5 < n < 4 \quad (48)$$

The corresponding range of $\langle A \rangle$ depends on the accepted value of $\sigma[A]$. The decision about the appropriate amplitude and its dispersion can be made from analysis of $n_{obs} - \tau_{ch}$ diagram provided above. Indeed, according to estimation (30), typical relative deviations ε are as high as $0.7 \div 0.8$, which corresponds to the $\sigma[A] \sim 0.1$ in Figure 10. So, we believe that the most adequate choice is:

$$0.5 < \langle A \rangle < 0.8, \quad (49)$$

and

$$\sigma[A] \sim 0.1 \quad (50)$$

Obtained values of n are in a good agreement with the $n = 3$ expected from simple magnetodipolar pulsar braking theory with constant (or slowly evolving) K (Manchester & Taylor 1977).

The median evolutionary trend, assuming $n = 3$, relative $\dot{\nu}$ amplitude $\langle A \rangle = 0.65$ and $\sigma[A] = 0.1$, is shown in Figure 4.

4.8 Timescales of cyclic process

The model of observed pulsars' spin-down does not include explicit relation between variational phase φ , pulsar age and timescale of variations T . To estimate the distribution of T , we will formulate it separately. Namely, let

$$\varphi = \varphi_0 + \Omega t, \quad (51)$$

where $\Omega = 2\pi/T = const.$

Since functions $\varepsilon(t)$ and $\eta(t)$ defined earlier are not fully independent and related through equation (13), the timescales (or frequencies) of a variational process for our model may be estimated directly: assuming secular spin-down law (31), $\varepsilon = A \cos \varphi = A \cos(\Omega t + \varphi_0)$, $\dot{\varepsilon} = -\Omega A \sin(\Omega t + \varphi_0)$, for each pulsar:

$$\Omega = -\frac{\dot{\nu} n_{obs}(1 + A \cos \varphi) - n}{A \sin \varphi}, \quad (52)$$

To get the distribution of *all* possible Ω 's for the observed set we simulated uniformly distributed phases φ , as well as values of n and A – according to probability distributions within the confidence regions derived in Section 4.7. Negative Ω values were rejected during this simulation as corresponding to physically impossible combinations of parameters. Distribution of Ω simulated for $\sigma[A] = 0.1$ is shown in Figure 11. Corresponding timescales are clustered inside a 5 – 500 thousands of years region.

Also, the Figure 11 displays theoretical distribution for the timescales of NS precession caused by an anomalous braking torque (see Section 5.2 and equation (57)) for comparison. These timescale values depend on a number of physical parameters of NS, such as surface magnetic field, initial

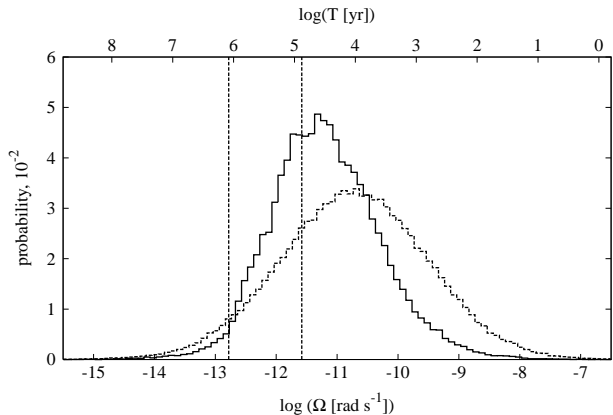


Figure 11. The distribution of a timescales of long-term variations, estimated according to the observed pulsars’ frequency and its derivatives, for spin-down parameters values derived in Section 4.7 (see text for details). The timescales are clustered around 5 – 500 thousands of years and are in a good agreement with similar distribution of NS precession timescales caused by anomalous braking torque (dotted line, see Section 5.2). Dashed lines represent timescales T_{up} and T_{tyP} according to estimations (19) and (24), respectively, for $\dot{\nu} = 10^{-14} \text{ s}^{-2}$.

period etc. We used distributions of B and P_0 derived by Faucher-Giguère & Kaspi (2006): $\log B$ and P_0 distributed normally with $\langle \log B[G] \rangle = 12.65$, $\sigma_{\log B} = 0.55$, $\langle P_0 \rangle = 0.3$ s and $\sigma_{P_0} = 0.15$ s. Masses and radii of NS have been taken distributed uniformly within 1.3 – 1.6 M_\odot and 8 – 12 km intervals, respectively. Initial magnetic dipole angles have been chosen randomly from $[0; \pi/2]$ interval.

Both obtained distributions are in a good agreement with each other and consistent with the idea of a long-term thousands-of-years variations of a pulsars’ timing parameters.

5 DISCUSSION

In this work we revise the problem of anomalous values of isolated radiopulsars braking indices. Since individual values of $\dot{\nu}$ are strongly dominated by non-monotonous component of the spin-down, we performed a statistical analysis of the ensemble of 297 objects. As a result, we concluded that pulsars’ behaviour on the $\dot{\nu} - \nu$ and $\ddot{\nu} - \nu$ diagrams suggest the existence of long-term cyclic mechanism affecting observed timing parameters. We constructed a semi-phenomenological model of observed pulsar spin-down and estimated it parameters.

We found that the timescale of the $\dot{\nu}$ long-term variations is likely close to few thousands of years – it follows both from simple model-independent estimation (Section 3.4) and from accurate maximum likelihood analysis (Section 4.8).

In general, our analysis inevitably suggests that observed $\dot{\nu}$ of radiopulsars vary with large enough relative amplitude. As a result, basic pulsar parameters depending on $\dot{\nu}$ may be significantly over- or underestimated. We already said some words about this effect in Section 3.5, and below we’ll continue its discussion.

5.1 Ages of young pulsars revised

Let’s return to the diagram $n_{obs} - \tau_{ch}$ (Fig. 7). There are eight pulsars in area III with $n_{obs} > 0$, associated with young supernova remnants. Assuming their n_{obs} are biased mostly due to $\dot{\nu}$ variations, i.e. $\eta = 0$, corresponding instant ε can be derived as

$$\varepsilon = \sqrt{3/n_{obs}} - 1 \quad (53)$$

Therefore, their evolutionary characteristic ages

$$\tau_{ch,ev} = \tau_{ch}(1 + \varepsilon) \quad (54)$$

and magnetic fields

$$B_{ev} = \frac{B}{\sqrt{1 + \varepsilon}}, \quad (55)$$

where B is according to equation (27), can be estimated, which are expected to be closer to the physical ones.

We analysed data on three of these eight supernova remnants that have more or less independent and confident estimations of their ages, and summarized the results in Table 1. In general, corrected pulsars’ ages become more consistent with that of corresponding SNRs in all of these cases. While the estimations of magnetic fields in all cases exceed 10^{13} G. At the same time, if one assume initial periods P_0 for these pulsars, then the same corrections of characteristic ages can be provided by the proximity of the P_0 and the current period.

A similar correction for the pulsars of area I is not so evident. Whether the measured $n_{obs} < 3$ of the youngest Crab-like pulsars are indeed biased from evolutionary $n = 3$ due to the same variational process is not clear. However, according to equation (29), pulsars born with nonzero characteristic ages $P_0/2K \sim 10^3$ years. If so, then all pulsars in area I likely have $\tau_{ch,ev}$ greater than at least 2 thousands of years while their measured $\tau_{ch} < 2$ kyr imply positive ε .

We believe that understanding of a possibility of significant biasing of standard estimators of pulsars’ ages will induce new insights on the PSR-SNR connections, evolution and kinematics.

5.2 Long timescale precession of a neutron star?

And finally we will discuss possible physical nature of a long-term variations of observed pulsars’ spin-down suggested in this work.

The unusual timescale of these variations – thousands of years – is much larger than the pulsar rotational period and, on the other hand, much shorter than its typical lifetime. At the same time, even the canonical magnetodipolar braking model seems to already include an essential mechanism for long-term variations.

More than half a century ago Deutsch (1955) derived the vacuum solution for the electromagnetic field of a perfectly conducting, rigidly rotating spherical star. The full braking torque affecting such a star with magnetic moment $\vec{\mu}$ and spin angular velocity $\vec{\omega}$ may be described as a superposition of three orthogonal terms (in observer’s frame):

$$\dot{\vec{\omega}} = \alpha \cdot (\vec{\mu} \times \vec{\omega}) + \beta \cdot ((\vec{\mu} \times \vec{\omega}) \times \vec{\omega}) + \gamma \cdot \vec{\omega} \quad (56)$$

where $\mu = const$. The second and third components of this braking torque are due to the magnetodipolar radiation in

Table 1. Corrections for characteristic ages and magnetic fields of several pulsars due to $\dot{\nu}$ variations. Here ε is an estimated relative $\dot{\nu}$ shift assuming evolutionary braking index $n = 3$ and $\delta\dot{\nu} = 0$, while P_0 is an initial pulsar period that is necessary to provide the same correction.

PSR	τ_{ch}, yr	B, G	ε	$\tau_{ch,ev}, \text{yr}$	B_{ev}, G	SNR	SNR age, yr	P_0, s
B1853+01	2×10^4	7.6×10^{12}	-0.50	10^4	1.1×10^{13}	W44	10^4 [1]	0.190
B2334+61	4×10^4	9.9×10^{12}	-0.46	2.1×10^4	1.3×10^{13}	G114.3+0.3	$(1 - 2) \times 10^4$ [2]	0.346
B1758-23	60×10^3	7.0×10^{12}	-0.89	6.6×10^3	2.1×10^{13}	W28	$(2.5 - 150) \times 10^3$ [3,4]	0.391

[1] Rho et al. (1994)

[2] Fich (1986)

[3] Long et al. (1991)

[4] Kaspi et al. (1993)

far (wave) zone. Both of them vary as $(\omega R/c)^3$, where R is the star radius (Davis & Goldstein 1970). At the same time, first component of torque (56) is due to radiation in near zone and varies as $(\omega R/c)^2$. Since $\omega R/c \approx 10^{-4} - 10^{-2}$ for a typical pulsar, the near-field torque is up to four orders of magnitude greater than far-field one.

However, being very strong, this torque does not directly affect pulsar spin-down rate and can not change magnetic inclination angle χ , as it is always perpendicular to both rotational and magnetic axes, in contrast to the far-field part of the torque driving the evolution of pulsar' ω and χ (Davis & Goldstein 1970).

This near-field torque induces an additional complex rotation of the star. Indeed, first term of torque (56) describes a precession of a neutron star around its magnetic axis with angular frequency $\Omega = |\alpha\mu|$. Due to the strength of the near-field torque, the characteristic timescale of this precession is significantly shorter than the pulsars' typical lifetime. Precisely, in a simple vacuum magnetodipolar case, precession period remains constant and is equal to (Good & Ng 1985)

$$T = \frac{2\pi}{\Omega} = (2.9 \times 10^3 \text{ yr}) \cdot I_{45} \cdot \nu_{i,50}^{-1} \cdot B_{s,12}^{-2} \cdot R_6^{-5} \cdot \cos^{-1} \chi_0 \quad (57)$$

Here ν_i – pulsar's initial frequency normalized to 50 Hz; $B_{s,12}$ – surface magnetic field normalized to 10^{12} G; I_{45} – NS moment of inertia normalized to $10^{45} \text{ g} \cdot \text{cm}^2$, and R – NS radius normalized to 10^6 cm ; χ_0 – initial magnetic inclination angle. The value of $\Omega \ll \omega$ depends strongly on the NS parameters, hence one can expect a wide range of precession periods, from hundreds to thousands years. The distribution of these periods for reasonable values of NS parameters is shown in Figure 11 and is in a good agreement with estimations of variational process timescales derived in this work.

Note, that similar long-term precession on a timescales of few thousand years can be also caused by the NS distortion along the magnetic axis due to the strong magnetic field (Goldreich 1970).

However, if we associate pulsar beam symmetry axis with NS magnetic moment then it is possible to show that such NS precession itself can not cause large observed deviations of $\ddot{\nu}$ (and $\dot{\nu}$) – moreover, it is unable to power a cyclic variations in observed NS spin-down rate at all. Indeed, the braking torque vector (56) is dominated by the strong near-field term. Hence, assuming $\beta \approx 0$ and $\gamma \approx 0$:

$$\dot{\vec{\omega}} \approx \alpha \cdot (\vec{\mu} \times \vec{\omega}) = (\vec{\Omega} \times \vec{\omega}), \quad (58)$$

where Ω is a constant precession frequency. At the same

time, observed pulsar spin frequency is defined by rotation of $\vec{\mu}$. However, this vector rotates around angular velocity $\vec{\omega}$:

$$\dot{\vec{\mu}} = (\vec{\omega} \times \vec{\mu}), \quad (59)$$

which also changes its direction relative to observer. Therefore, the value of *observed* spin frequency of $\vec{\mu}$ is not equal to ω and is not clear from equations (58) and (59) only.

But, combining these two equations we found that $\dot{\vec{\omega}} + \alpha\dot{\vec{\mu}} = 0$, which suggests introduction of the vector

$$\vec{L} = \vec{\omega} + \alpha\vec{\mu} = \vec{\omega} + \vec{\Omega} = \text{const} \quad (60)$$

which is useful for the description of $\vec{\mu}$ rotation by a simpler equation similar to (59):

$$\dot{\vec{\mu}} = (\vec{L} \times \vec{\mu}) \quad (61)$$

Since $\vec{L} = \text{const}$, it is clear that a star precessing around its magnetic axis looks like a non-precessing star with a bit biased observed spin frequency

$$L \approx \omega + \Omega \cos \chi, \quad (62)$$

where χ is a magnetic inclination angle.

Therefore, even slow *monotonous* evolution of Ω , ω and χ are unable to introduce any irregularities in observed spin-down rate. The discussed type of precession is indiscernible for an observer.

Therefore, if observed long-term spin-down variations are really caused by such precession, some geometrical or physical mechanism connecting rotation of $\vec{\omega}$ around $\vec{\mu}$ with modulation of χ , $\dot{\omega}$ etc should be suggested.

Thus, Barsukov & Tsygan (2010) considered an alteration of electric currents in the NS magnetosphere caused by such precession, which leads to modulation of $\dot{\omega}$. At the same time, Melatos (2000) have shown that for non-spherical but biaxial or triaxial NS, near-field torque will strongly affect its rotation. If pulsar's rotational axis (and magnetic moment) significantly deviates from the one of its main inertia axes, then a very large variations of χ (and consequently of $\dot{\omega}$) occur. However, variations so large are not observed (Melatos 2000).

Generally, any change in the observed pulsar timing parameters are determined by the variations of the $d\psi/dt$, where ψ is the dihedral angle between two planes – the plane of symmetry axis of a pulsar beam and the plane formed by rotational axis and direction to the observer. Detailed investigations of observed complex timing behaviour should always take into account the geometry of pulsar emission.

Ultimately, whether the monotonous precession of NS rotation axis around the magnetic moment able to produce any non-monotonous peculiarities in observed $\dot{\nu}$ and $\ddot{\nu}$ is not clear, but at least this process operates on sufficiently long timescales of thousands of years. On the other hand, there are no obvious physical reason behind some hypothetical stochastic process with ultra-red spectrum, able to produce the same amplitude of pulsars' second derivatives variations. The regular nature of these variations seems phenomenologically preferable.

6 CONCLUSIONS

In this work we analysed the properties of a set of 297 “ordinary” radio pulsars with a well detected, via a pulsar timing, second frequency derivative. As a result we demonstrate that

- the long term spin-down of pulsars is well described by the superposition of a “true” monotonous and a long timescale non-monotonous cyclic term;
- the subsets of these pulsars with positive and negative second derivatives are statistically different, both in shape and in number of objects; this effect is stronger for younger pulsars and vanishes for the older ones;
- this difference reflects the existence of an evolutionary, secular positive trend $\ddot{\nu}_{ev}$; the $\ddot{\nu}$ variations around this trend are nearly symmetric;
- simple binomial arguments based on the assumption of symmetric variations around the evolutionary trend allow to construct reliable estimator for pulsars' long-term spin-down parameters;
- pulsars secular spin down is consistent with a classical magnetodipolar braking with $n \approx 3$
- the mean relative amplitude of the first frequency derivative ($\dot{\nu}$) variations is as large as $\langle A \rangle = 0.5 - 0.8$ with variance $\sigma[A] \approx 0.1$
- the characteristic timescale of these variations is likely to be of several thousands years;
- consequently, the observed values of pulsars' characteristic age are biased by the factor of 0.5 – 5 from the “true” secular value $\tau_{ch,ev}$; this fact naturally explains the discrepancy between real ages and characteristic ages of several pulsars associated with supernova remnants, the presence of pulsars with extremely large, up to $\sim 10^8$ years, characteristic ages, and low braking indices of the youngest pulsars.
- there is at least one physical reason able to produce such variations in magnetodipolar model – a complex neutron star rotation relative its magnetic axis due to influence of the near-field part of magnetodipolar torque.

ACKNOWLEDGMENTS

This work has been supported by the Russian Foundation for Basic Research (Grant No. 04-02-17555), Russian Academy of Sciences (program “Evolution of Stars and Galaxies”), by the Russian Science Support Foundation, by the Grant of President of Russian Federation for the support of young Russian scientists (MK-4694.2009.2) and by the grant of Dynasty foundation. The authors are grateful to the anonymous Referee for his/her thoughtful review which lead to significant improvement of the paper.

REFERENCES

- Alpar, M. A., Baykal, A., 2006, MNRAS, 372, 489–496
- Arzoumanian, Z., Nice, D. J., Taylor, J. H. et al., 1994, ApJ, 422, 671–680
- Barsukov, D.P., Tsygan, A.I., 2010, MNRAS, 409, 1077–1087
- Baykal, A., Ali Alpar, M., Boynton, P. E. et al., 1999, MNRAS, 306, 207–212
- Beskin, V., Gurevich, A. & Istomin, Ya., 1993, Physics of the Pulsar Magnetosphere, Cambridge: Cambridge University Press.
- Bhattacharya, D., Wijers, R. A. M. J., Hartman, J. W., Verbunt, F., 1992, A&A, 254, 198–212.
- Beskin, G., Biryukov, A., Karpov, S., 2006, astro-ph/0603375
- Biryukov, A., Beskin, G., Karpov, S. & Chmyreva, L., 2007, AdSpR, 40, 1498–1504
- Cardiel, N., 2009, MNRAS, 396, 680–695
- Cheng, K.S., 1987, ApJ, 321, 799
- Chukwude, A.E., 2003, A&A, 406, 667–671
- Chukwude, A.E., 2007, Chin. J. Astron. Astrophys., 7, 521–530
- Cordes, J. M. & Helfand, D.J., 1980, ApJ, 239, 640
- Cordes, J. M. & Downs, G. S., 1985, ApJS, 59, 343–382
- Cordes, J. M. & Greenstein, G., 1981, ApJ, 245, 1060–1079
- Cordes J.M. & Lazio, T.J.W., 2002, arXiv:astro-ph/0207156
- Cordes, J. M. & Shannon, R.M., 2010, arXiv:1010.3785
- Contopoulos, I., 2007, A&A, 475, 639–642
- D’Alessandro, F., McCulloch, P. M., King, E. A. et al., 1993, MNRAS, 261, 883–894
- Davis, L., Goldstein, M., 1970, ApJ, 159, L81–L86
- Demiański, M., Proszynski, M., 1979, Nature, 282, 383–385
- Deutsch, A., 1955, Ann. d’Ap., 18, 1–10
- Edwards, R. T., Hobbs, G. B. & Manchester, R. N., 2006, MNRAS, 372, 1549–1574
- Espinoza, C. M., Lyne, A. G., Stappers, B. W., Kramer, M., 2011, MNRAS 414, 1679–1704
- Faucher-Giguère, C.-A., Kaspi, V. M., 2006, ApJ, 643, 332–355
- Fich, M., 1986, ApJ, 303, 465
- Goldreich, P., Julian, W. H., 1969, ApJ, 157, 869–880
- Goldreich, P., 1970, ApJ, 160, L11–L15
- Good, M. L. & Ng, K.K., 1985, ApJ, 299, 706–722
- Gullahorn, G. E., Rankin, J. M., 1977, Bull. of the Am. Astro. Soc., 9, 562
- Hill, T. P., Miller, J., 2010, arXiv:1005.4978
- Hill, T., 2011, Trans. of Am. Math. Soc., 363, 3351–3372
- Hobbs, G., Lyne, A. G., Kramer, M. et al., 2004, MNRAS, 353, 1311–1344
- Hobbs, G., Lyne, A. G., Kramer, M., 2010, MNRAS, 402, 1027–1048
- Johnston, S., Galloway, D., 1999, MNRAS, 306, L50
- Kaspi, V. M., Lyne, A. G., Manchester, R. N., Johnston, S., D’Amico, N., Shemar, S. L., 1993, ApJ, 409, L57–L60.
- Livingstone, M. A., Kaspi, V. M., Gavriil, F. P., Manchester, R. N., 2005, ApJ, 619, 1046–1053
- Long, K. S., Blair, W. P., Matsui, Y., White, R. L., 1991, ApJ, 373, 567–578.
- Lyne, A. G., Pritchard, R. S. & Smith, F. G., 1993, MNRAS, 265, 1003–1012.

- Lyne, A., 1999, in: Arzoumanian Z., van der Hooft F. & van den Heuvel E. P. J. (Eds.), Amsterdam, p.141
- Lyne, A., Hobbs, G., Kramer, M. et al., 2010, *Science*, 329, 408
- Manchester, R. N., Hobbs, G. B., Teoh, A. et al., 2005, *AJ*, 129, 1993–2006
- Manchester, R. N. & Taylor, J. H., 1977, *Pulsars*, San Francisco: Freeman
- Melatos, A., 2000, *MNRAS*, 313, 217–228
- Rho, J., Petre, R., Schlegel, E. M., Hester, J. J., 1994, *ApJ*, 430, 757–773
- Scott, D.M., Finger, M.H. & Wilson, C.A., 2003, *MNRAS*, 344, 412
- Tauris, T.M. & Manchester, R.N., 1998, *MNRAS*, 298, 625–636.
- Urama, J.O., Link, B., & Weisberg, J. M., 2006, *MNRAS*, 370, L76–L79